Nigerian Research Journal of Engineering and Environmental Sciences 8(1) 2023 pp. 268-276
p ISSN: 2635-3342; e ISSN: 2635-3350

Nigerian Research Journal of Engineering and Environmental Sciences
Journal homepage: www.rjees.com

Original Research Article

Prediction of Pile Bearing Resistance in Multi-Layered Soil using Optimality Criterion

Ike, V.I.

Department of Civil Engineering, Faculty of Engineering, Nigeria Maritime University, Okerenkoko, Warri, Nigeria.
ike.vincente@gmail.com; vincent.ike@nmu.edu.ng

http://doi.org/10.5281/zenodo.8095112

ARTICLE INFORMATION

Article history:
Received 04 Apr. 2023
Revised 18 May 2023
Accepted 19 May 2023
Available online 30 Jun. 2023

Keywords:
Optimal load
Pile foundation
Multi-layered soil
Pile bearing capacity
Tapered pile
Elastic boundary conditions

ABSTRACT

This paper discusses the problem of designing a pile foundation in a multi-layered soil that optimizes the buckling load, taking into consideration the stiffness and frictional resistances of the soil strata. The optimality criteria method was applied in the context of Rayleigh's quotient, and solved for by variational principles with associated boundary conditions. The results revealed the minimum buckling load of the tapered pile on the multi-layered soil, the resultant effect on the elastic boundary condition. A numerical illustration is presented to emphasize the impact of the pile's tapering and shaft friction, soil non-uniformity, pile-soil stiffness, and the boundary condition at both ends of the pile. It is expected that the study will furnish geotechnical and structural engineers with a tool to easily predict strength improvements in pile foundations from any known layered soil medium.

1. INTRODUCTION

Pile foundations can suffer from buckling, which can compromise their stability and load-bearing capacity. Buckling occurs when a pile is subjected to an axial compressive load that causes it to deflect laterally, leading to a loss of stability and a reduction in load-carrying capacity. Factors that can contribute to pile buckling include the length and diameter of the pile, the soil conditions (stiffness and thickness of each soil layer), the magnitude and direction of the applied loads, and the stiffness of the surrounding soil (Muhammad, et al., 2022). Pile buckling is more likely to occur in long, slender piles with a low stiffness and in soft soils that can undergo significant deformation. To prevent pile buckling, it is important to design the pile foundation system to take into account the specific soil. Optimizing the buckling load of a pile in a multilayered soil is an important consideration in the design of pile foundations to ensure improvements in the load-carrying capacity of the structure (Luigi et al., 2021).

Buckling of slender foundation elements is a common concern among designers and structural engineers. Ofner and Wimmer (2007) and Vogt *et al.* (2009) in their research showed that buckling of piles is subject to the soils' strength properties. Their study supports the resolve that buckling in soil is tenable in weak region of soil strength such as peat, very loose sands, erodible soil, liquefiable soil, and soft clay.

A great deal of work has settled on the strength of pile stability in single layered soil system (Yang and Song, 2000; He *et al.*, 2003; Hurd and Truman, 2006; Li and Wang, 2014). However, studies have been made over the years in an attempt to integrate the conclusion in multilayered soil profiles. Gabr, *et al.* (1997) developed a pile buckling model assuming a general power distribution of the soil's horizontal subgrade reaction to represent various soil conditions. The minimum potential energy method was adopted to develop the model using the Rayleigh–Ritz method to select a suitable deflection function, and the effects of nine different boundary. Ofner and Wimmer (2007) extended buckling analysis of micropiles in homogeneous soils to micropiles driven into different soil layers. They based their assumptions on experimental buckling tests carried out on 4m long micropiles embedded in soft clay. Their research of pile-buckling calculations reveals a contrast between design codes application and computational FEM solver. Despite the fact that the study considered multi-layered soil, the calculations were done for each layer separately, and the softest soil layer was the only candidate for the buckling position. Bhattacharya, *et al.* (2009) extended the dynamic instability of piles in liquefiable soils. A correction factor was suggested to compensate for the natural frequency reduction of piles in a liquefied condition. Meyerhof and Purkayastha (2011) investigated various combinations of eccentricity and inclined loaded piles with varying thicknesses of clay layer. His research presented significant influence on the bearing capacity of single piles and pile group as a result of the thickness of clay layer in layered soil. Utilizing the differential transformation method, Vega-Posada *et al.* (2020) also showed the effects of high and low soil stiffness and intermediate boundary conditions on pile buckling behaviour. Fenu *et al.* (2021) proposed the eigenvalue-eigenvector approach in solving for the minimum buckling load and describing the pile deformation by a Fourier developed coefficients.

In addition, as pile applications continue to evolve and require higher capacity (i.e., higher allowable stress) of the pile cross section, the conventional design practices which assume that fully embedded piles will not buckle before the yielding of the pile cross section are no longer applicable (Vogt, *et al.*, 2009). In a previous study by Lee *et al.* (2015) examined how the tapering and cross-section shape of piles, held at a constant volume, can influence their buckling behavior. However, the analysis assumed that the axial load is constant along the pile and that no load transfer occurs along the pile shaft. This assumption is only applicable to relatively short, stubby, end-bearing piles. The buckling of friction piles can be affected by the shaft resistance along the pile, but only a few solutions exist that take this into account. For example, the energy method (Luigi et al., 2021), Rayleigh-Ritz method (Gabr *et al.*, 1994), and modal clustering technique (Heelis et al., 2004) have been used to analyze straight friction piles. More recently, Kai *et al.* (2020) studied the stability of a tapered friction pile in heterogeneous soils with assumptions of a linear stiffness and linear lateral friction resistance in the theoretical model. However, as far as the author is aware, the buckling load optimization of tapered friction piles has not been studied in the open literature.

The perspective of this research is to draw a qualitative and quantitative intuition in the stability and optimality of the pile foundation subject to a multi-layered soil distribution. The study applies optimality criteria method. The objective function is to minimize the compression load in the context of Rayleigh's quotient of the analytical model adopted from Heelis *et al.* (2004) and Sadiku (2010), and subject to the constraint of a fixed volume and height of the pile. Variational principles is suggested to reveal the behaviour of stability and optimality of the system, with concerns for the boundary conditions obtainable in such system, and to easily solve for the singularity functional of the interlayered soil in terms of stiffness and frictional resistances.

2. METHODOLOGY

2.1. Problem Formulation

The research problem in Figure 1 is to minimize the buckling load of the pile foundation while satisfying the volumetric constraints. Equation (1) is the objective function and minimum axial compressive force (N_{cr}) at the top of the pile foundation (Heelis et al., 2004)

$$N_{cr} = \min_{w(x)} \frac{\int_0^l \left\{ E\theta A\left(x\right)^n w_{xx}^2 + k\left(x\right) w^2 - f\left(x\right) w_x w \right\} dx}{\int_0^l w_x^2 dx} + \int_0^x f\left(x\right) dx \tag{1}$$

Where, w is the lateral deflection and x is the depth below the soil surface. Further, E is the modulus of elasticity of the pile. l is the length of the pile. θA^n is the second moment of area of the pile at any section - which is the product of the cross-sectional area A and the constants, θ and n. $k(x)$ is the modulus of subgrade reaction over the pile width, and $f(x)$ is the friction per unit length of pile. $k(x)$ and $f(x)$ are assumed to be subject to the soil property at any section as defined in Equation (2).

$$\begin{aligned} k\left(x\right) &= \sum_{i=1}^{m} k_i \times \left[H\left(x - \beta_{i-1} l\right) - H\left(x - \beta_i l\right) \right] \\ f\left(x\right) &= \sum_{i=1}^{m} f_i \times \left[H\left(x - \beta_{i-1} l\right) - H\left(x - \beta_i l\right) \right] \end{aligned} \tag{2}$$

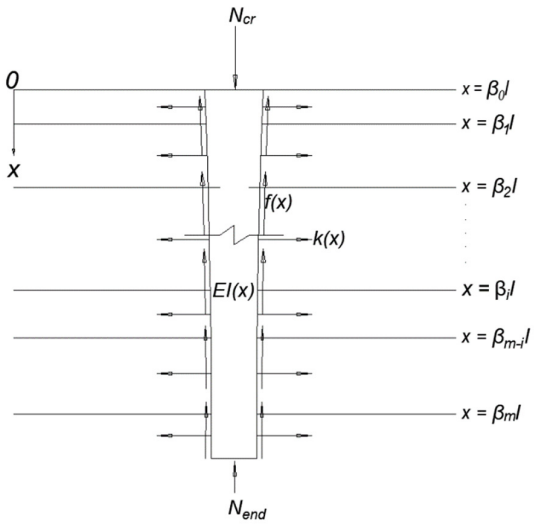

Figure 1: Pile foundation in multi-layered soil

H represent the Heaviside function and β_i are the depth ratios of the soil layered interfaces in terms of the thicknesses with respect to the entire strata. By introducing a volumetric constraint, the Lagrangian function is introduced to the minimization problem, and written as shown in Equation (3).

$$R(N_{cr}) = \min_{w(x)} \frac{\int_0^l \left\{ E\theta A\left(x\right)^n w_{xx}^2 + k\left(x\right) w^2 - f\left(x\right) w_x w \right\} dx}{\int_0^l w_x^2 dx} + \int_0^x f\left(x\right) dx + \lambda \left\{ V - \int_0^l A\left(x\right) dx \right\} \tag{3}$$

Where λ is the Lagrange multiplier and V is the fixed volume of the pile. A minimum of the Lagrangian is located where the derivatives with respect to the design variable A, and buckling variable w equals zero. Equation (4) is the design equation, which is the resolve of the derivative of Equation (3) with respect to A as:

$\delta R(A) \Rightarrow$

$$nE\theta A^{n-1}w_{xx}^2 = \lambda l\int_0^l w_x^2 dx = c^2 \tag{4}$$

Where c^2 represent such constant in the change in curvature of the axial plane. Similarly, Equation (5) represent the buckling equation, as the derivative of Equation (3) with respect to w:

$\delta R(w) \Rightarrow$

$$\int_0^l \left\{E\theta A^n w_{xx}\delta w_{xx} + kw\delta w - fw\delta w_x\right\}dx - \int_0^l \sigma_{cr} w_x \delta w_x dx = 0 \tag{5}$$

Noting that we have defined:

$$\sigma_{cr} = N_{cr} - \int_0^x f\left(x\right)dx \tag{6}$$

By applying variational principles, Equation (5) reduces to:

$$\int_0^l \left\{E\theta\left(A^n w_{xx}\right)_{xx} + kw + \left(fw\right)_x\right\}\delta w dx + \int_0^l \left(\sigma_{cr} w\right)_{xx}\delta w dx = 0 \tag{7}$$

And the corresponding boundary conditions, considering that the pile is fixed at bottom and elastically restraint at top:

$$\left.\begin{aligned} w\left(l\right) = w_x\left(l\right) = 0; \\ w_x + \frac{1}{k_1}\left[E\theta A^n w_{xx}\right]_x \\ w + \frac{1}{k_1}\left[E\theta(A^n w_{xx})_x + fw + \left(\sigma_{cr} w\right)_x\right]_x \end{aligned}\right| = 0; \quad \text{at } \beta_{i-1} l \le x \le \beta_i l \tag{8}$$

Where k_1 is the soil stiffness resistance at the top of the pile depth. By introducing dimensionless terms and noting Equation (6), Equation (4) and (7) becomes:

$$q_{ss}^2 = C^2; \tag{9}$$

$$(\alpha^n q_{ss})_{ss} + \eta kq + \gamma\left[\left(fq\right)_s - \left(hq\right)_{ss}\right] + P_{cr} q_{ss} = 0 \tag{10}$$

with Boundary conditions of Equation (8), and observing Equation (6):

$$\begin{gathered} q\left(-1\right) = q_s\left(-1\right) = 0; \\ q_s\left(\beta\right) + \frac{1}{\kappa_1}\left[\alpha^n q_{ss}\right]_{s=\beta} = q\left(\beta\right) + \frac{1}{\kappa_2}\left\{\left(\alpha^n q_{ss}\right)_s + \gamma\left[fq - \left(hq\right)_s\right] + P_{cr} q_s\right\}_{s=\beta} = 0; \\ \kappa_1 = \frac{k_1 l}{E\theta};\ \kappa_2 = \frac{k_1 l^3}{E\theta}; \end{gathered} \tag{11}$$

where β is the depth ratio of elastic restraint at the top of the pile.

Equation (9) through (11) is subject to the following dimensionless terms are introduced into Equation (4, 7 & 8):

$$s=\frac{x}{l},\alpha=\frac{A}{l^2},q=\frac{w}{l};w_{x}=q_{s},w_{xx}=\frac{q_{ss}}{l},w_{xxx}=\frac{q_{sss}}{l^2},w_{xxxx}=\frac{q_{ssss}}{l^3};$$
$$\eta=\frac{l^3}{E\theta},\gamma=\frac{l^2}{E\theta},C^2=\frac{c^2l^2}{E\theta},P_{cr}=\frac{N_{cr}}{E\theta};\tag{12}$$
$$k\left(x\right)=lk\left(s\right),f\left(x\right)=lf\left(s\right),\int_0^x f\left(x\right)dx=l^2\int_0^s f\left(s\right)ds=l^2h\left(s\right)$$

2.2. Analysis and Design

The problem of minimizing the buckling load in the layered soil can be easily approached by conventional method of solution when $n = 1$, which is a case of a plane tapered weight (axial) distribution in depth. Hence, by solving the design and buckling equations (9) and (10) respectively, and adopting the appropriate boundary conditions in Equation (11), the axial distribution becomes:

$$\alpha=\theta\left(s\right)-\frac{P_{cr}s^2}{2}+cs+d\tag{13}$$

Where c and d are constants of integration, and noting that

$$\theta\left(s\right)=\iint_s\left[2\gamma h_{s}s-\gamma\left(fs-h\right)-\gamma\left(f_{s}-h_{ss}\right)\frac{s^2}{2}-\eta k\frac{s^2}{2}\right]ds^2\tag{14}$$

Substituting Equation (13) into Equation (11), so that:

$$\beta c+d+\theta\left(\beta\right)-\frac{\beta^2}{2}P_{cr}=0;\;\; c+\frac{\beta^2}{2}\kappa_{2}+\frac{\gamma}{2}\left(\beta^2f-2\beta h\right)=0;\tag{15}$$

By solving the equation (15) simultaneously, and substituting the solution of the constants c and d into equation (13) becomes:

$$\alpha\left(s\right)=\left(\beta^2-s^2\right)\frac{P_{cr}}{2}+\theta\left(s\right)-\theta\left(\beta\right)+\left(\beta-s\right)\frac{\beta^2}{2}\kappa_{2}-\beta\kappa_{1}+$$
$$\gamma\left(\beta-s\right)\frac{\beta^2}{2}f\left(\beta\right)-\gamma\left(\beta-s\right)\beta h\left(\beta\right)\tag{16}$$

From Equation (3), one can draw perspective from the dimensionless volumetric constraint posed where:

$$\frac{V}{l^3}=\int_0^{-1}\alpha\left(s\right)ds\tag{17}$$

By integrating Equation (16) from zero to unity (1) of the dimensionless variable s, the resolve in Equation (17) suffices in the form:

$$\frac{V}{l^3}\Rightarrow\frac{\alpha}{l^2}=\frac{P_{cr}}{6}\left(1-3\beta^2\right)+\int_0^{-1}\left[\theta\left(s\right)-\theta\left(\beta\right)\right]ds-\frac{\kappa_{2}\beta^2}{4}\left(1+2\beta\right)+\beta\kappa_{1}+$$
$$\gamma\left[\frac{h\left(\beta\right)\beta}{2}\left(1+2\beta\right)-\frac{f\left(\beta\right)\beta^2}{4}\left(1+2\beta\right)\right]\tag{18}$$

Introducing the dimensionless terms from Equation (12) in terms of the buckling load, Equation (18) becomes:

$$N_{cr} = \frac{6E\theta}{\left(1-3\beta^2\right)}\left\{\frac{\alpha}{l^2} - \int_0^{-1}\left[\theta\left(s\right)-\theta\left(\beta\right)\right]ds + \frac{\kappa_2\beta^2}{4}\left(1+2\beta\right) - \beta\kappa_1 - \gamma\left[\frac{h\left(\beta\right)\beta}{2}\left(1+2\beta\right) - \frac{f\left(\beta\right)\beta^2}{4}\left(1+2\beta\right)\right]\right\} \tag{19}$$

Finally, Equation (19) reduces to:

$$N_{cr} = \frac{6}{\left(1-3\beta^2\right)}\frac{EI}{l^2} - \frac{6}{\left(1-3\beta^2\right)}\left\{\int_0^{-1}\left[\phi\left(s\right)-\phi\left(\beta\right)\right]ds - \frac{k_1\beta^2l^3}{4}\left(1+2\beta\right) + \beta k_1 l + l^2\left[\frac{h\left(\beta\right)\beta}{2}\left(1+2\beta\right) - \frac{f\left(\beta\right)\beta^2}{4}\left(1+2\beta\right)\right]\right\} \tag{20}$$

Where

$$\phi\left(s\right) = l^2\iint_s\left[2h_s s - \left(fs-h\right) - \left(f_s - h_{ss}\right)\frac{s^2}{2} - kl\frac{s^2}{2}\right]ds^2 \tag{21}$$

Equation (20) is the solution of the minimum buckling load of the pile in the multi-layered soil. This solution is subject to the condition that the pile is plane tapered from the top to the bottom so as to achieve optimal strength.

4. RESULTS AND DISCUSSION

To validate the report from Equation (20), a close reference is the buckling load for a uniform elastic system of same height *l*, constant volume of the material *V*, and a fixed-free boundary conditions (Case et al., 1999), which is:

$$N = 2.47\,EI/l^2 \tag{22}$$

Consider that the soil functional in Equation (20) is ignored (that is if the first terms from the right side equals zero), and ($\beta \to 0$) for a fixed-free case (in Figure 1). By interpolation technique, the improvement by the tapered effect can be found to be:

$$\frac{N_{cr}-N}{N} > \frac{6\,EI/l^2 - 2.47\,EI/l^2}{2.47\,EI/l^2} = 1.4291 \tag{23}$$

Equation (23) reveals that the optimal buckling load of the pile is 142.91% in excess of the corresponding uniform section in Equation (22) of same volume and height. This magnitude in improvement is a result of the tapered configuration.

It is common knowledge that:

$$N_{end} = \mu N_{cr} \tag{24}$$

Where N_{end} is the end bearing soil resistance (in Figure 1), μ represents the proportion of the buckling load which is supported at the base of the pile. In this way, piles completely supported by friction will have $\mu = 0$ and end bearing piles with no friction will have $\mu = 1$ (Heelis, *et al.*, 2004). The presentation considers a case of friction and end bearing pile support, hence $0 \le \mu \le 1$. That is, at any point along the individual soil layers, the resultant dimensionless friction functional, while observing Equation (2) and (12) will be

$$f(s)=\sum_{i=1}^{m}\frac{N_{cr}-N_{end}}{l}\times l\times\left[H\left(s-\beta_{i-1}\right)-H\left(s-\beta_{i}\right)\right]=\sum_{i=1}^{m}N_{cr}\left(1-\mu_{i}\right)\times\left[H\left(s-\beta_{i-1}\right)-H\left(s-\beta_{i}\right)\right]\quad\therefore\quad h(s)=lf(s)\tag{25}$$

and the resultant dimensionless stiffness functional at any point along the individual layers becomes

$$k(s)=\sum_{i=1}^{m}k_{i}\times l\times\left[H\left(s-\beta_{i-1}\right)-H\left(s-\beta_{i}\right)\right]\tag{26}$$

For the case under consideration, let the properties of the reinforced concrete pile be:

$$E=35GPa,\ l=25m,\ \theta=1/4\pi$$

Table 1 shows the interlayers of soil strata. Here, a five-layer composite of varying thickness is introduced and β_i is the depth ratios of the soil layered interfaces. k_i and μ_i are the coefficient of stiffness parameter and the proportion of sliding frictional resistance per layered soil respectively.

Table 1: Geotechnical data of the sample five-layer soil profile

Layer position, *i*	Soil type	Layer thickness (*m*)	Cumulative Depth (*m*)	β_i range	k_i, MPa	μ_i
1	Medium to dense sand	1.95	1.95	0.000 – 0.065	21.670	0.300
2	Soft to very soft sandy clay	4.95	6.90	0.065 – 0.230	8.330	0.174
3	Loose to medium dense sand	2.55	9.45	0.230 – 0.315	12.080	0.350
4	Medium to dense sand	14.55	24	0.315 – 0.800	38.330	0.370
5	Very dense sand	6.00	30	0.800 – 1.000	71.670	0.400

Figure 2 shows the solution of optimal shape (distribution) of the strongest tapered pile through the layered soils from equation (16). The elastic restraint at the top such that β is *-0.065* is introduced in contrast to a free end condition *(i.e. β = 0)*. The shape function is observed to follow a parabolic law. The condition of elastic restraint proved to have a lesser steepness than that when β is *zero*. The resultant reveals that stress distribution is reduced when elastic restraint is introduced in the system. The zero value at the top of the pile (i.e. s = 0) also showed the absence of disturbances from the layered soils capable of distorting the stress distribution of the tapered pile. It can be further noticed that the tapered configuration is gentle, hence, adequate for consideration in slender pile design.

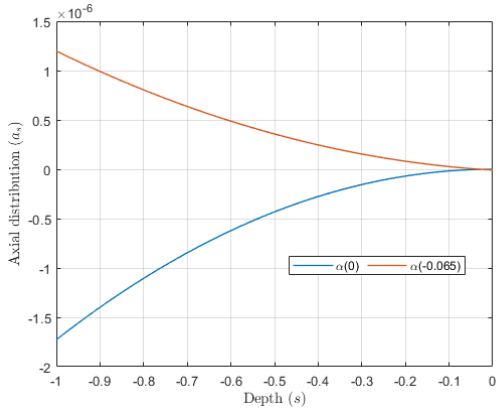

Figure 2: Optimal axial distribution of tapered pile in multi-layered soil

Table 2 shows the minimum buckling load in Equation (20) with piles of different sizes in the multi-layered soil described in Table 1. Two boundary cases are considered: the fixed-free boundary condition ($\beta \rightarrow 0$), and the fixed-elastic constraint condition ($\beta \rightarrow \beta_1$). β_1 is the depth ratio of the top soil that constitute the elastic restraint. The result showed the improvements of the minimum buckling load in the presence of layered soils when the pile size increases, or some elastic restraint is introduced at the top of the tapered pile.

Table 2: Minimum pile buckling load (k*N*) at *25m* of length

Boundary condition		Pile Diameter (*mm*)			
		400	600	800	1000
		Buckling Load (*kN*)			
$\beta \rightarrow 0$	with layered soils	422.23	2137.54	6755.68	16493.36
	without layered soils	422.23	2137.54	6755.68	16493.36
$\beta \rightarrow -0.065$	with layered soils	429.76	2167.09	6844.51	16707.20
	without layered soils	427.65	2164.98	6842.41	16705.10

4. CONCLUSION

The results of this work have revealed that the optimal weight distribution of a pile in a multi-layered soil medium is distributed by a parabolic curve. This parabolic functional is subject to the depth ratios, magnitude of the pile load, and the layered soils configuration. A contrast is drawn to highlight the improvement of the bearing capacity in the presence of elastic soil restraint.

5. CONFLICT OF INTEREST

There is no conflict of interest associated with this work.

REFERENCES

Bhattacharya, S., Adhikari, S. and Alexander, N. (2009). A Simplified Method for Unified Buckling and Free Vibration Analysis of Pile Supported Structures in Seismically Liquefiable Soils. *Soil Dynamics and Earthquake Engineering 29*, pp. 1220-1235.

Fenu, L., Congiu, E., Deligia, M., Giaccu, G. F., Hosseini, A. and Serra, M. (2021). Buckling Analysis of Piles in Multi-Layered Soils. *Applied Sciences*, *11*(22), 10624.

Case, J., Chilver, L. and Ross, C. (1999). Buckling of Columns and Beams. In *Strength of Materials and Structures (Fourth Edition)* (pp. 424-457). New York: John Wiley & Sons.

Gabr, M., Wang, J. and Kiger, S. (1994). Effect of boundary conditions on buckling of friction piles. *Journal of Engineering Mechanics 120(1)*, pp. 392-400.

Gabr, M., Wang, J. and Zhao, M. (1997). Buckling of Piles with General Power Distribution of Lateral Subgrade Reaction. *Journal of Geotechnical and Geoenvironmental Engineering 123*, pp. 123-130.

He, X., Zhou, L. and Wang, Q. (2003). Determination of critical buckling load of pile by finite element method. *Journal of Wuhan University of Technology, 25 (6)*, pp. 25-27.

Heelis, M. E., Pavlovic´, M. N. and West, R. P. (2004). The Analytical Prediction of the Buckling Loads of Fully and Partially Embedded Piles. *Geotechnique, 54(6)*, pp. 363-373.

Hurd, A. and Truman, K. (2006). Optimization Method of Pile Foundations. In M. Pandey, W. Xie, & L. Xu, *Advances in Engineering Structures, Mechanics & Construction* (pp. 653-661). Netherlands: Springer.

Kai, L., Junxiu, L., Xianfeng, S., Baoquan, C. and Guangyong, C. (2020). Study on Buckling Behavior of Tapered Friction Piles in Soft Soils with Linear Shaft Friction. *Advances in Civil Engineering*, pp. 87-96.

Lee, J., Kim, N. and Jeon, C. (2015). Dynamic stability analysis for Beck's type of inelastic Timoshenko steel columns. *International Journal of Steel Structures*, 15(4), pp. 959-971.

Li, Y. and Wang, J. (2014). Analysis of Buckling Stability of Deep and Long Foundation Pile. *Advanced Materials Research, 1049-1050*, pp. 438-441.

Luigi, F., Alireza, H., Mauro, S., Gian, F., Mariangela, D. and Eleonora, C. (2021). Buckling Analysis of Piles in Multi-Layered Soils. *Applied Sciences, 11(22)*, pp. 10-24.

MeyerhofR, G. G. and D., P. (2011). Ultimate Pile Capacity in Layered Soil under Eccentric and Inclined Loads. *Canadian Geotechnical Journal, 22(3)*, pp. 399-402.

Muhammad, H., Muhsiung, C., Pungky, D., Nina, P., Anasya, A., Sabrina, H. and Surya, D. (2022). Effects of various factors on behaviors of piles and foundation soils due to seismic shaking. *Solid Earth Sciences, 7(4)*, pp. 252-267.

Ofner, R. and Wimmer, H. (2007). Buckling Resistance of Micropiles in Varying Soil Layers. *Bautechnik, 84*, pp. 881-890.

Sadiku, S. (2010). On the Application of the Perturbation Method in the Buckling Optimization of a Heavy Elastic Column of Constant Aspect Ratio. *Journal of Optimization Theory and Applications, (146)*, pp. 181–188.

Vega-Posada, C., Gallant, A. and Areiza-Hurtado, M. (2020). Simple approach for analysis of beam-column elements on homogeneous and non-homogeneous elastic soil. *Engineering Structures*, pp. 11-25.

Vogt, N., Vogt, S. and Kellner, C. (2009). Buckling of slender piles in soft soils. *Bautechnik, 86*, pp. 98-112.

Yang, W. and Song, L. (2000). Axial buckling analysis for top-free and bottom-fixed pile. *Engineering Mechanics, 5(10)*, pp. 43-56.